

Superconducting Instability in the Periodic Anderson Model

A. N. Tahvildar-Zadeh, M. H. Hettler, M. Jarrell

Department of Physics, University of Cincinnati, Cincinnati, OH 45221-0011

(August 13, 2018)

Employing a quantum Monte Carlo simulation we find a pairing instability in the normal state of the infinite dimensional periodic Anderson model. Superconductivity arises from a normal state in which the screening is protracted and which is clearly not a Fermi liquid. The phase diagram is reentrant reflecting competition between superconductivity and Fermi liquid formation. The estimated superconducting order parameter is even, but has nodes as a function of frequency. This opens the possibility of a temporal node and an effective order parameter composed of charge pairs and spin excitations.

Introduction A number of Heavy Fermion materials display highly unusual superconductivity (Ott 1994, Grewe and Steglich 1991, Hess, Riseborough and Smith 1993). It seems unlikely that conventional superconductivity coexists with the strong local Coulomb correlations necessary to enhance the electronic mass in these systems. Indeed, the specific heat jump at the transition scales with the normal state specific heat making it clear that pairing is between the heavy electrons. However, strong Coulomb correlations present no problem for unconventional superconducting order parameters with either spatial (Sauls 1994) or temporal (Berezinski 1974, Balatsky and Abrahams 1992, Abrahams 1995) nodes. The latter can occur with either odd or even-frequency order parameters, which are interpreted in terms of composite condensates (Bonca and Balatsky 1994). Such an interpretation is supported by two sets of data: (i) power laws observed in physical properties below the superconducting transition (Ott 1994, Sauls 1994), which contrast with the activated behavior of the conventional (nodeless) s -wave order of, e.g., lead; (ii) the complex superconducting phase diagrams of UPt_3 and $\text{U}_{1-x}\text{Th}_x\text{Be}_{13}$ (and possibly UBe_{13} itself, for which the penetration depth displays evidence of a secondary transition) (Ott 1994, Sauls 1994). Finally, at least in UBe_{13} (Ott 1987) and CeCu_2Si_2 (Steglich 1996), the superconductivity arises in a normal state which is clearly *not* a Fermi liquid. For $T \gtrsim T_c$ in each of these materials, the linear specific heat (C/T) rises with decreasing T while the resistivity decreases and has a high residual value at T_c (typically 80-100 $\mu\Omega\text{-cm}$ in the best samples of UBe_{13}).

We have recently analyzed some static (Tahvildar-Zadeh, Jarrell and Freericks 1997a) and dynamic (Tahvildar-Zadeh, Jarrell and Freericks 1997b) properties of two theoretical paradigms of heavy fermion materials: the single-impurity Anderson model (SIAM) and the periodic Anderson model (PAM). We found for metallic systems with an f -band filling $n_f \approx 1$ and d -band filling $n_d \lesssim 0.8$, the Kondo scale for the PAM, T_0 , is strongly suppressed compared to T_0^{SIAM} , the Kondo scale for a SIAM with the same model parameters. Consequently,

the temperature dependence of the Kondo peak in the f spectral function is protracted in the PAM, i.e. it is much weaker than in the SIAM, consistent with experiments on single-crystalline Kondo lattice materials (Andrews 1996). However the high temperature ($T > T_0^{\text{SIAM}}$) properties of the two models are similar, so that T_0^{SIAM} is still the relevant scale for the onset of screening in the PAM whereas T_0 , which bears no obvious relation to T_0^{SIAM} , is the scale for the onset of coherence where the moment screening is almost complete and the Fermi liquid begins to form.

We interpreted our results as indicating the emergence of a single heavy band described by an effective Hubbard model for the local screening clouds introduced by Noziers (Noziers 1985). Since the effective model is close to half filling and its hopping constant is strongly suppressed by the overlap of the screened and unscreened states of the f -electron moments, its Kondo scale, T_0 , becomes much less than T_0^{SIAM} . In this paper, we show that the regime of protracted screening is also associated with the occurrence of a pairing instability in the PAM.

Formalism The PAM Hamiltonian on a D -dimensional hypercubic lattice is,

$$H = \frac{-t^*}{2\sqrt{D}} \sum_{\langle ij \rangle \sigma} \left(d_{i\sigma}^\dagger d_{j\sigma} + \text{H.c.} \right) + \sum_{i\sigma} \left(\epsilon_d d_{i\sigma}^\dagger d_{i\sigma} + \epsilon_f f_{i\sigma}^\dagger f_{i\sigma} \right) + V \sum_{i\sigma} \left(d_{i\sigma}^\dagger f_{i\sigma} + \text{H.c.} \right) + \sum_i U (n_{fi\uparrow} - 1/2)(n_{fi\downarrow} - 1/2) . \quad (1)$$

where $d(f)_{i\sigma}^\dagger$ destroys (creates) a $d(f)$ electron with spin σ on site i . The hopping is restricted to the nearest neighbors and scaled as $t^*/2\sqrt{D}$. U is the screened on-site Coulomb repulsion for the localized f states and V is the hybridization between d and f states. We choose t^* as the unit of energy ($t^* \approx$ a few electron-volts, the typical band-width of conduction electrons in metals).

We solve this model Hamiltonian with the dynamical mean field (DMF) method of Metzner and Vollhardt

(Metzner and Vollhardt 1989) who observed that the irreducible self-energy and vertex-functions become purely local as the coordination number of the lattice increases. As a consequence, the solution of an interacting lattice model in $D = \infty$ may be mapped onto the solution of a local correlated impurity coupled to a self-consistently determined host (Pruschke, Jarrell and Freericks 1995; Georges, Kotliar, Krauth and Rozenberg 1996). We employ the quantum Monte Carlo (QMC) algorithm of Hirsch and Fye (Hirsch and Fye 1989) to solve the remaining impurity problem and calculate the imaginary time, local, one and two particle Green's functions. The maximum entropy method (Jarrell and Gubernatis 1996) can then be used to find the f and d density of states and the self-energy.

We search for pairing between the f -electrons by calculating the f -electron pair-field susceptibility in the normal state. As shown in Fig. 1, this may be re-expressed in terms of the pairing matrix \mathbf{M} following Owen and Scalapino (Owen and Scalapino 1971). \mathbf{M} is formed from the irreducible superconducting (particle-particle, opposite-spin), local vertex function Γ_{sc} , and the bare pair susceptibility $\chi^0(i\omega_n, \mathbf{q}) = \sum_{i\omega_m, \mathbf{k}} G(i\omega_m, \mathbf{k}) G(i\omega_n - i\omega_m, \mathbf{q} - \mathbf{k})$, with $G(i\omega_m, \mathbf{k})$ the fully dressed lattice propagators;

$$\mathbf{M} = \sqrt{\chi^0(i\omega_n, \mathbf{q})} \Gamma_{sc}^{n,m} \sqrt{\chi^0(i\omega_m, \mathbf{q})}. \quad (2)$$

The total pair susceptibility in terms of \mathbf{M} is given by

$$P^{sc}(T) = \sum_{n,m} \sqrt{\chi^0(i\omega_n, \mathbf{q})} (1 - \mathbf{M})^{-1} \sqrt{\chi^0(i\omega_m, \mathbf{q})}. \quad (3)$$

For the usual second order normal-superconducting transition T_c is obtained when the largest eigenvalue λ of \mathbf{M} reaches one, so that the pair susceptibility diverges. The corresponding eigenvector $\Phi(i\omega_n)$ yields information about the superconducting order parameter. The pair-field susceptibility in this most singular channel can be projected out, using an appropriate frequency form factor $f_n = \Phi(i\omega_n) / \sqrt{\chi^0(i\omega_n, \mathbf{q})}$,

$$P_\lambda(T) = \sum_{n,m} f_n \left[\sqrt{\chi^0(\mathbf{q})} (1 - \mathbf{M})^{-1} \sqrt{\chi^0(\mathbf{q})} \right]_{n,m} f_m. \quad (4)$$

Results and Interpretation We introduce an effective hybridization strength $\Gamma(\omega)$,

$$\Gamma(\omega) = \text{Im} \left(\Sigma(\omega) + \frac{1}{G_f(\omega)} \right), \quad (5)$$

where $G_f(\omega)$ is the local f Green's function and $\Sigma(\omega)$ is the local f -electron self-energy. $\Gamma(\omega)$ is a measure of the hybridization between the effective impurity in the DMF problem and its medium (for example, in the SIAM $\Gamma(\omega) = \pi V^2 N_d(\omega)$, where $N_d(\omega)$ is the d -band density of

states). Fig. 2 shows the effective hybridization for the PAM near the Fermi surface $\mu = 0$. In this figure the model parameters are chosen to be $U = 1.5$, $V = 0.6$, $n_f \approx 1$ and three different d band fillings $n_d = 0.4$ ($T_0 = 0.014$), $n_d = 0.6$ ($T_0 = 0.054$) and $n_d = 0.8$ ($T_0 = 0.16$). A relatively small value of U/V^2 was chosen for presentation purposes; however, the features shown are also present for larger values of U/V^2 . (For the parameter set of Fig. 2 we do not observe any superconducting instability, although the hybridization functions look qualitatively very similar to the case where the instability exists).

The feature we want to emphasize on is the dip in $\Gamma(\omega)$ at the Fermi energy which develops as the temperatures is lowered. Since only the electronic states within about T_0 of the Fermi surface participate in the screening (Nozieres 1985) this indicates a reduced number of available screening states at the Fermi energy, and since the dip becomes narrower as $n_d \rightarrow 1$, the effect is more dramatic for small n_d . Thus, as the temperature is lowered and $n_d < 0.9$, the Kondo scale of the DMF effective impurity problem is self-consistently suppressed and hence the ‘‘coherence’’ Kondo scale T_0 is also suppressed. Concomitant with this suppression, the Kondo length scale $l_K \sim 1/T_0$ of the Kondo spin and charge correlations will increase dramatically. We have seen previously that these correlations can induce ferromagnetism in the PAM (Tahvildar-Zadeh *et al.* 1997a) and superconductivity in the two-channel Kondo model (Jarrell, Pang and Cox 1997).

As discussed in the previous section, a second order superconducting transition is indicated when the largest eigenvalue of the pairing matrix exceeds unity. However, in our calculation, the largest positive eigenvalue does not approach unity for any value of U or temperature studied. Instead, for relatively large values of $U \gtrsim 2t^*$ we see a different type of instability: At a high temperature ($T > t^*$) we find generally that all eigenvalues are either small in magnitude or large and negative. As the temperature is lowered, the positive eigenvalues grow slowly; however, the most negative eigenvalue diverges at a temperature T_u^* . Upon lowering the temperature further, the dominant eigenvalue (that with the largest absolute value) switches sign and becomes large ($\gg 1$) and positive. It then decreases for some range of temperatures, but eventually increases again, diverges at a temperature T_l^* , and switches back to large and negative. The corresponding pair susceptibility $P_\lambda(T)$ goes continuously through zero at the temperatures $T_{u(l)}^*$ of the divergence of the dominant eigenvalue λ . $P_\lambda(T)$ is negative for $T_l^* < T < T_u^*$, indicating a pairing instability of the system in this channel. We find that these instabilities are degenerate throughout the Brillouin zone, i.e., $P_\lambda(T = T_{u(l)}^*)$ vanishes for every \mathbf{q} over the whole zone. We demonstrate this by plotting the corresponding *local*

pair susceptibility $P_\lambda^{local}(T)$ in Fig. 3 and observe that the instability prevails even at the local level. Hence this is a *locally* driven transition, consistent with a transition driven by local dynamical correlations such as those responsible for Kondo screening. We suspect that the degeneracy in the Brillouin zone will be lifted in a finite D calculation by non-local dynamical correlations, such as spin waves, as has been suggested previously (Jarrell, Pang and Cox 1997).

To understand how the vanishing of the pair susceptibility indicates a phase transition, remember that the inverse pair susceptibility is proportional to the curvature of the free energy $f(\Delta)$ as a function of the pair order parameter Δ , $1/P_\lambda(T) \propto d^2 f(\Delta)/d\Delta^2$. Thus, if $P_\lambda(T) < 0$ the normal state becomes thermodynamically unstable. The associated transition cannot be continuous, since this would require $f(\Delta)$ to become flat for small Δ (i.e. $P_\lambda(T)$ diverges) so that the order parameter may change continuously. Thus the observed transition is *discontinuous*. Furthermore, if $P(T_u^*) = 0$, then T_u^* is a lower bound to the transition temperature since when $P_\lambda(T - T_u^* = 0^-) = 0^-$ the curvature of $f(\Delta)$ is divergent and negative, i.e. the free energy displays an upward cusp. This would compel the order parameter and the free energy to change discontinuously at T_u^* , which involves an infinite energy at the transition. Hence, the actual transition occurs at a temperature $T_c > T_u^*$. Similar arguments can be made to show that T_l^* is an upper bound to the discontinuous transition back to the normal metal.

The dominant eigenvector of the pairing matrix at $T = T^*$ is even in frequency but has both positive and negative parts. To show the effect of the nodes on the order parameter in the ordered phase, we first introduce the Nambu-Gorkov matrix form for the local f-Green's function

$$\mathbf{G}_f(i\omega_n) = \sum_{\mathbf{k}} \frac{1}{i\omega_n Z_n \mathbf{I} - \epsilon_f \tau_3 - \phi_n \tau_1 - \frac{V^2}{[i\omega_n \mathbf{I} - (\epsilon_k + \epsilon_d) \tau_3]}} \quad (6)$$

where \mathbf{I} , τ_1 and τ_3 are Pauli matrices. $Z_n = 1 - \text{Im}(\Sigma(i\omega_n))/\omega_n$ is the wave function renormalization factor and ϕ_n is the renormalized gap function. The f-electron order parameter is given by $G_{f12}(\tau)$, the Fourier transform of the off-diagonal component of $\mathbf{G}_f(i\omega_n)$. In order to study this order parameter using our knowledge of the normal state, we assume that ϕ_n has the same temporal parity as the dominant eigenvector of the pairing matrix \mathbf{M} right at $T = T^*$ (in the normal phase). But we are not able to predict its actual value by this assumption. Hence, as the simplest approximation, we assume that $\phi_n = cf_n$ where c is an unknown real normalization factor and f_n is the form factor constructed from the dominant eigenvector of the pairing matrix at $T = T^*$. As c increases, $G_{f12}(\tau)$ de-

velops a suppression at $\tau = 0$ (inset of Fig. 3). An order parameter with $G_{f12}(0) \approx 0$ corresponds to a condensate which excludes the simultaneous occupation of the same site by two electrons, minimizing its Hubbard energy. For the large values of $U \gtrsim 2t^*$ where an instability is observed, we therefore assume that the condensate with $G_{f12}(0) \approx 0$ is the most stable one. For small τ , an order parameter corresponding to an even-frequency ϕ_n takes the form $G_{f12}(\tau) \approx \Delta_0 + \frac{1}{2}\Delta_2\tau^2$. If $\Delta_0 = \langle f(\tau = 0^+)f(\tau = 0) \rangle = 0$, then the superconducting condensate is characterized by $\Delta_2 \propto \langle [[f, H], H]f \rangle$. In the strong-coupling limit, where the system can be mapped onto the Kondo lattice model, the commutators bring spin operators into the average (Bonca and Balatsky 1994), and if $\Delta_0 = 0$, the order parameter is effectively a composite of charge pairs and spin-excitations. Such an order parameter is compelling as it relates naturally to the complex phase diagram of the superconducting heavy-fermion materials, in which the competition and sometimes coexistence of antiferromagnetism and superconductivity is observed. However, it is unclear whether our estimate corresponds to the actual order parameter of the broken symmetry state. A Monte Carlo simulation in the broken symmetry state is presently underway.

Fig. 4 shows the resulting superconducting phase diagram for the PAM with parameters $U = 2$, $V = 0.5$ and $n_f \approx 1$. The symbols correspond to the temperature where the pairing susceptibility $P_\lambda(T)$ crosses zero and the largest diverging eigenvalue changes sign as discussed above. Note that the instabilities cease for $n_d \gtrsim 0.9$, leading to a phase diagram which suggests re-entrance into the normal state. Since T_l^* is only an upper bound to T_c^l , an actual re-entrance transition need not occur, i.e. T_c^l could be vanishing. On the other hand, this would require the upper transition temperature (which is bounded from below by T_u^*) to drop from a rather large value to zero upon a minute increase of n_d . Although we cannot rule this out numerically, we believe this scenario to be unlikely. The upper part of Fig. 4 shows the Kondo scale for the PAM and SIAM with the same model parameters as stated above. We see that the superconducting instability occurs only when $T_0 < T_0^{SIAM}$, i.e., in the “protracted screening” regime. This again suggests that the pairing mechanism is related to underscreened moments and Kondo physics. Note that the upper transition temperature is large, as is often the case for a mean field theory. We expect the non-local dynamical correlations of a finite dimensional system to significantly reduce our estimate for T_u^* . Also, as noted previously (Tahvildar-Zadeh, Jarrell and Freericks, 1997) the protracted screening regime and the associated superconductivity vanish when the orbital f-degeneracy diverges. Thus, these phenomena are associated with finite orbital degeneracy.

The shape of the lower phase boundary of the transi-

tion back to the normal metal is consistent with the n_d dependence of the “coherent” Kondo scale T_0 . This indicates that with the complete screening of the local moments below T_0 the system either loses the mechanism driving superconductivity, or that the system can gain more free energy by forming a Fermi liquid. The shape of the upper phase boundary is more difficult to understand. T_u^* increases upon lowering n_d , in contrast to the simultaneous decrease of the impurity Kondo scale T_0^{SIAM} . Hence, the onset of local moment screening alone (described roughly by T_0^{SIAM}) does not lead to superconducting correlations. As observed by Nozieres (Nozieres 1985), there are not enough states near the Fermi surface to completely screen all of the f-moments, especially as the d-band filling decreases. It is compelling to relate T_u^* to the temperature where the conduction band states available for screening are exhausted. Then, for $T < T_u^*$, correlated lattice effects, such as superconductivity or the magnetic polarons described by Nozieres, are required to quench the relatively large entropy associated with the unscreened moments. Better understanding of these correlations will be essential in a more quantitative explanation of the observed superconducting phase.

Some understanding of these correlations is provided by examining the Matsubara frequency structure of the vertex function $\Gamma_{sc}(i\omega_n, i\omega_m)$ which is *minus* the effective interaction (e.g. to lowest order in perturbation theory $\Gamma_{sc}(i\omega_n, i\omega_m) \approx -U$). Fig. 5 shows Γ_{sc} corresponding to the point **b** in the phase diagram of Fig. 4 (**b** is just inside the superconducting region). $\Gamma_{sc}(i\omega_n, i\omega_m)$ is large and positive, indicating an attractive interaction, only at small frequencies, and it displays a central minimum. The width of the peak at each n_d is roughly $2\pi T_u^*$, which we have argued above to be related to Nozieres’ “exhaustion” energy scale. Thus, the energy scale inferred from the susceptibility data is also present in the vertex function. This again hints to Kondo/Nozieres screening as the mechanism driving the superconductivity.

Fig. 6 shows the irreducible superconducting vertex function in the $\omega_n = \omega_m$ direction ($\Gamma_{sc}(i\omega_n, i\omega_n)$) at three different points of the phase diagram (cf. Fig. 4). We generally find that the vertex function is purely negative for points outside the superconducting region such as **c**, whereas it has positive values at low frequencies for points inside the superconducting region such as **a** and **b**. This means that the effective interaction between particles of opposite spin is *attractive* for the points inside the superconducting phase, but it is *repulsive* in the normal phase. Furthermore, the narrow width and the dip in the vertex function around zero frequency signifies that the *attractive* interaction is highly retarded. The central dip almost becomes a node at points well within the superconducting phase (such as **a**) indicating that the static component of the attractive interaction is not significant. Therefore, the system would not gain energy by pairing

two electrons on the same site at the same time. This is consistent with a node in the order parameter $G_{f12}(\tau)$ at $\tau = 0$ as discussed above.

Conclusions In conclusion, we have found a pairing instability in the infinite-dimensional periodic Anderson model which we interpret as a superconducting instability. This instability has several unusual features including: (i) A reentrant phase diagram reflecting competition between superconductivity and Fermi liquid formation; (ii) For most of the phase diagram, the upper transition temperature $T_u^* \gg T_0$, indicating that superconductivity arises from a normal state which is clearly not a Fermi liquid; (iii) Although even in frequency, the dominant eigenvector of the pairing matrix has nodes, which opens the possibility of a composite order parameter with a temporal node; (iv) The superconducting instability occurs only in the protracted screening regime, where the effective hybridization diminishes and the Kondo length increases with decreasing temperature; (v) Within the superconducting regime, the vertex function displays a narrow feature with central node at low frequencies, consistent with a highly retarded interaction with a weak static component. These features, together with the fact that the instability occurs simultaneously over the whole zone (i.e., is locally driven), suggests that the pairing mechanism has its origins in the spin and charge correlations associated with Kondo/Nozieres screening of the f-electron spins.

We would like to acknowledge stimulating conversations with A. Arko, A.V. Balatsky, A. Chattopadhyay, D.L. Cox, J.K. Freericks H.R. Krishnamurthy, T. Pruschke, P.G.J. van Dongen and F.C. Zhang, and in particular D.W. Hess. This work was supported by NSF grants DMR-9704021 and DMR-9357199. Computer support was provided by the Ohio Supercomputer Center.

-
- [1] E. Abrahams, *et al.*, Phys. Rev. B **52**, 1271 (1995).
 - [2] A. B. Andrews *et al.*, Phys. Rev. B **53**, 3317 (1996).
 - [3] A.V. Balatsky and E. Abrahams, Phys. Rev. B **45**, 13125 (1992);
 - [4] V.L. Berezinski, JETP Lett. **20**, 287 (1974).
 - [5] J. Bonca and A.V. Balatsky, JETP Lett. **59**, 216 (1994).
 - [6] A. Georges, G. Kotliar, W. Krauth, and M. Rozenberg, Rev. Mod. Phys. **68**, 13 (1996).
 - [7] N. Grewe and F. Steglich, *Handbook on the Physics and Chemistry of Rare Earths*, Eds. K.A. Gschneidner, Jr. and L.L. Eyring (Elsevier, Amsterdam, 1991) Vol. 14, P. 343.
 - [8] D. W. Hess, P. S. Riseborough, J. L. Smith, *Encyclopedia of Applied Physics* Eds. G. L. Trigg (VCH Publishers Inc., NY), Vol. **7** (1993) p. 435.

- [9] J.E. Hirsch and R.M. Fye, Phys. Rev. Lett. **56**, 2521 (1989).
- [10] M. Jarrell and J.E. Gubernatis, Physics Reports Vol. **269** No.3, p133-195, (May, 1996).
- [11] M. Jarrell, H. Pang, and D.L. Cox, Phys. Rev. Lett. **78**, 2000 (1997).
- [12] W. Metzner and D. Vollhardt, Phys. Rev. Lett. **62**, 324 (1989).
- [13] P. Nozieres, Ann. Phys. Fr. **10**, 19-35 (1985).
- [14] H.R. Ott, J. Low Temp. Phys. **95**, 95, (1994).
- [15] H.R. Ott, Progress in Low Temperature Physics **6**, 21 5 (1987).
- [16] C. Owen and D. J. Scalapino, Physica **55**, 691(1971).
- [17] T. Pruschke, M. Jarrell and J.K. Freericks, Adv. in Phys. **42**, 187 (1995).
- [18] J.A. Sauls, Adv. in Phys. **43**, 113-141 (1994).
- [19] F. Steglich *et al.*, Physica **B223&224**, 1 (1996).
- [20] A.N. Tahvildar-Zadeh, M. Jarrell and J.K. Freericks, Phys. Rev. **B55**, R3332 (1997).
- [21] A. N. Tahvildar-Zadeh, M. Jarrell and J.K. Freericks, preprint cond-mat/9710136.

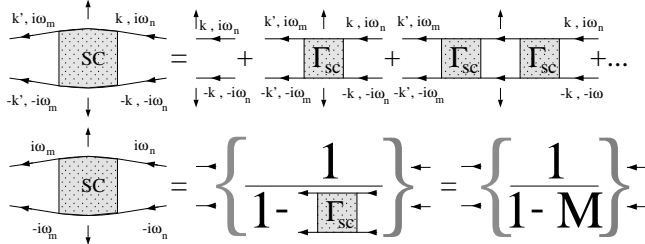


FIG. 1. Owen and Scalapino's pairing matrix formalism (Owen and Scalapino 1971). The diagrams for the pair-field susceptibility (top) after integration over the internal momenta may be re-written (bottom) in terms of the pairing matrix $\mathbf{M} = \sqrt{\chi^0} \Gamma_{sc} \sqrt{\chi^0}$ (Eq. 2). Here Γ_{sc} is the irreducible two-particle self energy matrix and χ^0 the bare pairing susceptibility. The square root is indicated by displaying only "half" of the electron Green's functions in the appropriate places. Second order phase transitions are signaled when the largest eigenvalue of \mathbf{M} reaches unity. The corresponding eigenvector Φ yields information about the superconducting order parameter.

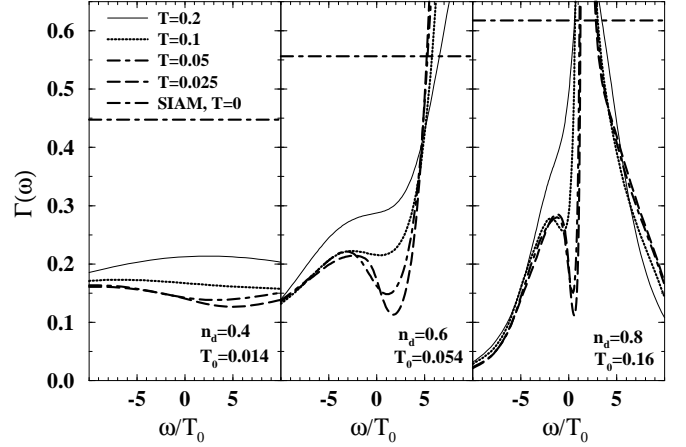


FIG. 2. Near-Fermi-energy ($\mu = 0$) structure of hybridization function for the asymmetric PAM. The model parameters are $U = 1.5$, $V = 0.6$ and $n_f \approx 1$. The dip at the Fermi-energy denotes a decrease in the number of states available for screening, leading to a suppressed "coherence" Kondo scale T_0 . The zero temperature hybridization for the single impurity model is shown for comparison.

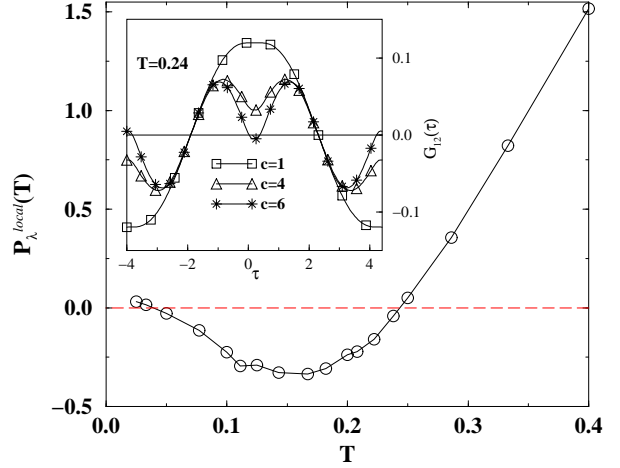


FIG. 3. The local pair susceptibility of the dominant eigenvalue versus temperature for the PAM with $U = 2$, $V = 0.5$, $n_d = 0.6$ and $n_f \approx 1$. The susceptibility $P_\lambda^{local}(T)$ is positive in the temperature regimes $T > T_u^*$ and $T < T_l^*$. It goes smoothly through zero at $T_{u/l}^*$ and would be negative in between, indicating an instability in the corresponding pairing channel. The eigenvalue λ diverges and changes sign at $T_{u/l}^*$ (not shown). The corresponding eigenvector has both positive and negative parts. The inset shows the corresponding superconducting order parameter $G_{f12}(\tau)$ calculated at $T_u^* \approx 0.24$ as described in the text. Since ϕ_n has arbitrary normalization, we multiply it by a parameter c . As c increases, the order parameter develops a suppression at $\tau = 0$. This indicates that the two elements of the pair are not on the same site at the same time, minimizing the Hubbard energy of the condensate.

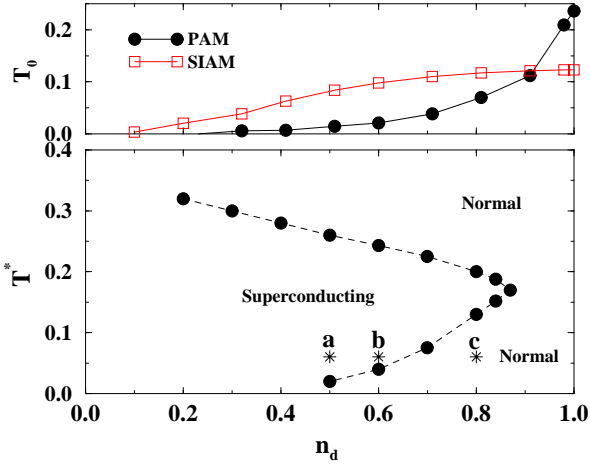


FIG. 4. Superconducting phase-diagram versus the d-band filling n_d (bottom) for the PAM with $U = 2$, $V = 0.5$ and $n_f \approx 1$. The symbols denote the upper and lower bounds for the region where the leading eigenvalue of the pairing matrix \mathbf{M} diverges (see text). The dashed line is a guide to the eye. The upper part shows the Kondo scales for the PAM and SIAM with the same parameters as for the lower part. Note that superconductivity only occurs where the lattice scale is suppressed relative to the impurity scale, and that the upper instability temperature $T_u^* > T_0^{PAM}$, indicating that the superconductivity emerges from a state which is not a Fermi liquid.

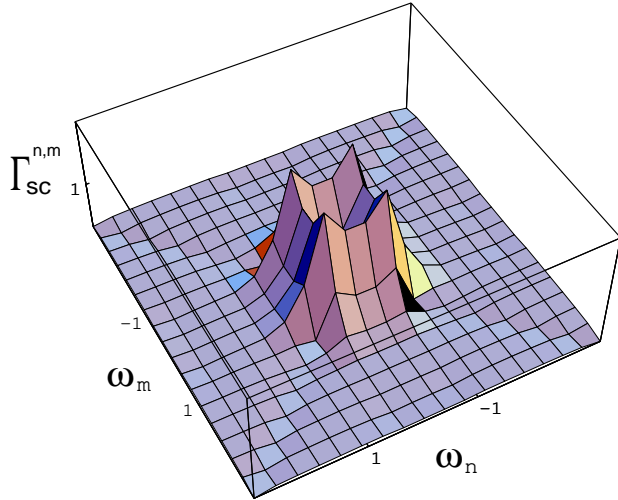


FIG. 5. The superconducting vertex function corresponding to the point **b** of Fig. 4. The z axis is in units of the function value at the central minimum. Note that the vertex function is large only at low frequencies, with a width $\omega_n \approx 2\pi T_u^*$.

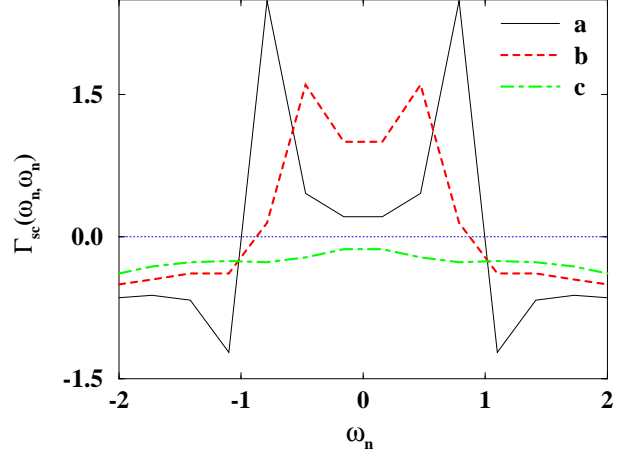


FIG. 6. The superconducting vertex function in $\omega_n = \omega_m$ direction at three different points of the phase diagram (cf. Fig. 4). The vertex function is purely negative for point **c** outside the superconducting region whereas it has positive values at low frequencies for points **a** and **b** inside the superconducting region, illustrating the attractive pair interaction in this region. Note that the narrow peak width and the dip around zero frequency implies strong retardation of the interaction.